Appendices

Appendix A: The method of the image charges applied to EFM of a dielectric layer with bottom electrode

A ferroelectric sample with a bottom electrode and a conductive SFM tip represent an electrostatic system for which the potential distribution and the electric field have to be determined. In this section, the method of the image charges is used to estimate, in a first approximation, the potential distribution produced by the application of a voltage between the SFM tip and the bottom electrode.

In first approximation, the spontaneous polarization is neglected and the ferroelectric is replaced with a dielectric medium (further referred to as M2) having the permittivity ε_2 and a thickness d. Also, the conductive tip in contact with the dielectric is replaced with a point charge q_0 at a distance h above the surface in the adjacent medium (denominated M1) having the permittivity ε_1. The bottom electrode, in contact with M2 on the opposite side of M1, is kept at zero potential. The solution of the simplified problem is based on the fact that the potential produced by q_0 has one equipotential surface which is tangential to the M1-M2 interface, and this surface may be considered as the surface of the tip.

For determining the potential inside the layer, the solution to two simple electrostatic problems turn out to be useful. The first one is the problem of a point charge located in M1 at a distance h from the plane that separates M1 from M2. This problem is further referred to as "DD" ("dielectric-dielectric"). The second elementary problem is that of a charge in front of an infinite conductive plane, from now on denominated "CP" ("conductive plane"). Both problems are solved in any basic course of electrostatics [181], and the respective solutions will be taken as known.

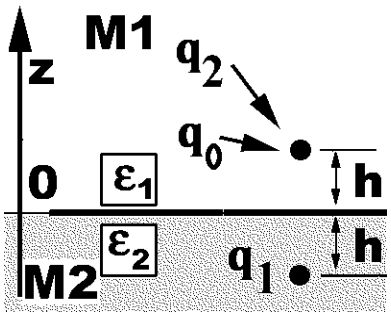

Figure A 1 Problem DD: A point charge in a medium M1 at a distance h of the surface that separates M1 and M2.

The solution of problem DD (the geometry of which is schematically represented in Figure A 1) is as follows: In M1 the potential is generated by two charges: a charge q_0 at $z = h$ in M1, and a charge q_1 at $z = -h$, in M2. In M2 the potential is given by a charge q_2 located in M1, at the same place as q_0. The values of the charges q_1 and q_2 are :

$$\begin{cases} q_1 = -q_0 \dfrac{\varepsilon_2 - \varepsilon_1}{\varepsilon_1 + \varepsilon_2} \\ q_2 = q_0 \dfrac{2\varepsilon_2}{\varepsilon_1 + \varepsilon_2} \end{cases} \qquad \textit{Eq. A 1}$$

The problem CP is trivial: the potential distribution of a system composed of a charge in front of a conductive plane is the same as the one of the initial charge plus a charge of opposite sign located symmetrically with respect to the plane.

For the initial problem, the origin of the axis z was chosen at the conductive plane, as shown in Figure A 2. The solution is based on successive imaging of charges with respect to the conductive plane and to the M1-M2 interface. The resolution of the problem can be performed following the succeeding steps:

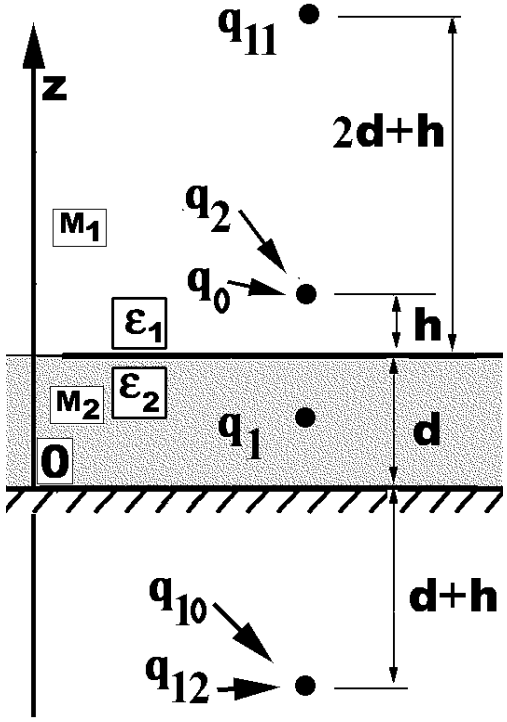

Figure A 2 Charges and their positions for the first two steps of the solution.

Step 1

The charge q_0 is imaged with respect to the dielectric interface (DD). In M1 the potential is given by q_0, at position $z_0 = (d + h)$ and by q_1 (according to problem DD) at position $z_1 = (d - h)$ (the origin is now at the conductive plane). In M2, the potential is given by the charge q_2 (according to problem DD), at position $z_2 = (d + h)$. The solution of the problem DD ensured the fulfillment of the boundary condition at the M1–M2 interface. Since the conductive plane *exists* beneath M2, and since *in* M2 the potential is given by the charge q_2 (*only,* for now), it follows that q_2 has to be imaged with respect to the conductive plane. This third charge $q_{10} = -q_2$ is located at the position $z_{10} = -(d + h)$, symmetric to that of q_2 with respect to the conductive plane (Figure A 2).

The "occurrence" of the charge q_{10} contributes to the potential in M2 (according to the problem CP) and thus the boundary condition of DD ceases to be satisfied! Therefore, the

imaging process has to start again, now with the initial charge q_{10} instead of q_0 (that's why it was called q_{10} and not q_3, for example).

Step 2

The new charge q_{10} (acting in M2, and which does not fulfill the boundary conditions of the previous solution of DD) is now the starting point of a new DD problem. The initial charge now being in M2 (and not in M1 as it was in the first DD problem), two other new charges are created. At this stage, the potential in M2 is given by the charges q_2 and q_{10}, and additionally, by the image charge q_{11} at position $z_{11} = d + (2d + h)$ (symmetric with respect to the dielectric interface). The potential in M1 is given, at this stage, by the charge q_{12} at position $z_{12} = -(d + h)$ (the same as q_{10}, according to the problem DD), in addition to the charges q_0 and q_1 (charges which were found previously that were acting in M1).

The values of the new charges are given in Eq. A 2 (the permittivities ε_1 and ε_2 of the solution DD in Eq. A 1 are interchanged, since now the initial charge is in M2).

$$\begin{cases} q_{10} = -q_2 = -q_0 \dfrac{2\varepsilon_2}{\varepsilon_1 + \varepsilon_2} \\ q_{11} = -q_{10} \dfrac{\varepsilon_1 - \varepsilon_2}{\varepsilon_1 + \varepsilon_2} \\ q_{12} = q_{10} \dfrac{2\varepsilon_1}{\varepsilon_1 + \varepsilon_2} \end{cases} \qquad \textit{Eq. A 2}$$

At this stage, the boundary conditions at the dielectric interface are fulfilled again, but with the new charge q_{11} acting in M2, the boundary condition at the conductive plane is not satisfied anymore, and this charge is the initial charge of a new CP problem. As a consequence, a new charge, $q_{20} = -q_{11}$, at $z_{20} = -(d + 3d + h)$, will contribute to the potential in M2, and the boundary conditions at the M1-M2 interface cease to be fulfilled.

Now the situation is the same as before in *Step 2*, with q_{20} being the starting charge. To find the complete solution, *Step 2* has to be repeated until the boundary conditions at the interfaces are fulfilled. It is important to note that no additional singularities are introduced by the imaging procedure: all the charges acting in M1 (M2) are located outside M1 (M2).

After performing the necessary calculations, the general formula for all image charges and their positions can be derived as given in Eq. A 3. The potential function is given in Eq. A 4. In these equations, k represents the number of *Step 2* iterative operations performed.

$$\begin{cases} q_0^k = (-1)^{2k-1} \left(\dfrac{\varepsilon_1 - \varepsilon_2}{\varepsilon_1 + \varepsilon_2} \right)^{k-1} \dfrac{2\varepsilon_2}{\varepsilon_1 + \varepsilon_2} q_0 \quad , \quad z_0^k = -\left[(2k-1)d + h \right] \\ q_1^k = -\dfrac{\varepsilon_1 - \varepsilon_2}{\varepsilon_1 + \varepsilon_2} q_0^k \quad , \quad z_1^k = z_0^k \\ q_2^k = \dfrac{2\varepsilon_1}{\varepsilon_1 + \varepsilon_2} q_0^k \quad , \quad z_2^k = (2k+1)d + h \end{cases} \qquad \textit{Eq. A 3}$$

$$\begin{cases} V_{M1} = V_0 + V_1 + \sum_{k=1} V_1^k \\ V_{M2} = V_2 + \sum_{k=1} (V_0^k + V_2^k) \end{cases} \qquad \textit{Eq. A 4}$$

In Eq. A 4, $V_\alpha^{(k)}$ is the potential produced by the charge $q_\alpha^{(k)}$, where $\alpha = 0$, 1, and 2. It is to be noted that the absolute values of the image charges are decreasing as k increases. Since the location of the charges is moving away from the interface with increasing k, the problem converges is rather rapidly, depending on the ratio between the two permittivities. For example, if $\varepsilon_2 / \varepsilon_1 \to \infty$ only the first step is needed and the electric field does not penetrate into M2. Usually, for $\varepsilon_2 / \varepsilon_1 = 100$ (a usual case for ferroelectric thin films) k = 5 iterations are needed to fulfill the boundary conditions with an accuracy of 1%.

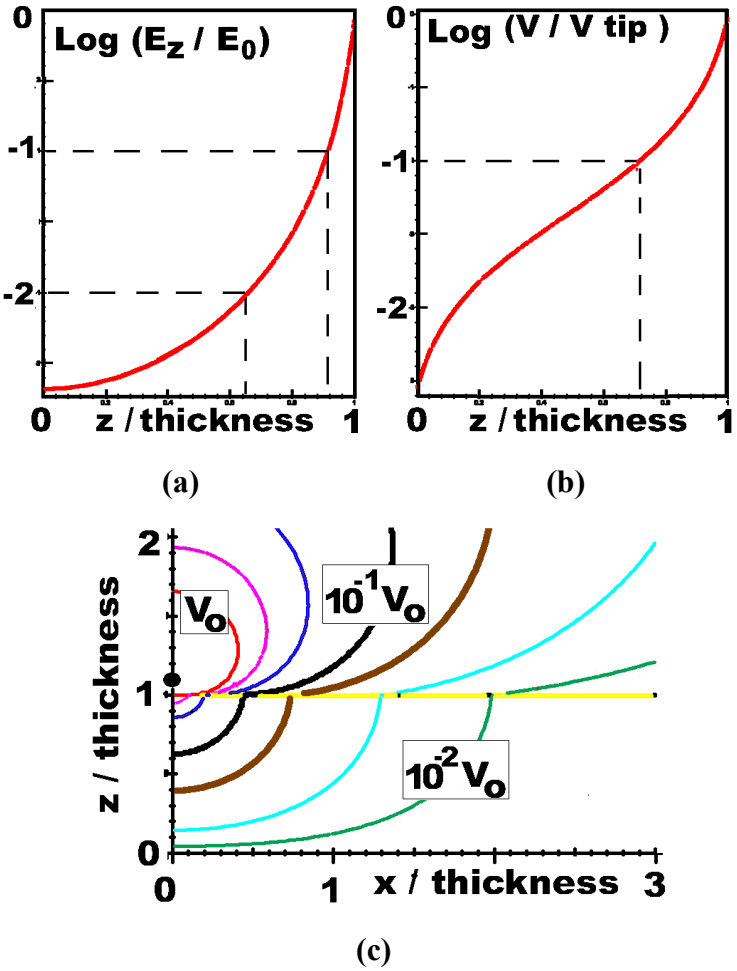

Figure A 3 (a, b) Electric field (a) and potential (b) versus position along the film thickness directly under the tip. **(c)** Cross-section normal to the film plane showing the equipotential surfaces. V_0 denotes the equipotential tangent to the surface, that may play the role of the tip surface (i.e. the voltage applied to the tip with respect to the bottom electrode). The distances in the plots are divided by the film thickness. Note: the accuracy is better than 1% (the potential at the bottom electrode is not zero, but less than 1% of the value at the surface).

The results of the calculations of the electric field and of the potential in the regions of interest for $\varepsilon_2 / \varepsilon_1 = 100$ are shown in Figure A 3. As expected, both the electric field and the potential inside the dielectric are extremely inhomogeneous and concentrated under the tip apex. The plot in Figure A 3a shows that the electric field at a depth of 35% of the

dielectric thickness under the surface is about 1% of the value at the contact place, and is ten times smaller than at a depth of 10% of the dielectric thickness. The potential plot in Figure A 3b shows that the voltage drop over the first 30% of thickness of the dielectric is almost 90% of the voltage applied to the tip.

Figure A 3c illustrates the equipotential surfaces in a cross-section through the y = 0 plane. Both *x*- and *z*-axes were scaled to the film thickness, so that the *z = 0* plane represents the dielectric-bottom electrode interface, whereas the sample surface is at z = 1. The presence of a field component parallel to the sample surface, in the near vicinity of the tip should be especially emphasized. This in-plane component may polarize the ferroelectric along radial directions parallel to the film surface. Whether or not the resulting domain structure is stable, depends on the material and on the local environment.

Appendix B: Dependence of the piezoelectric coefficients on the testing directions

In piezoresponse SFM, the tip senses the induced oscillations in a ferroelectric sample. If the spontaneous polarization is normal to the film plane, then the piezoelectric coefficient involved is the standard one. For example, if the sample probed is *c*-oriented PZT, the piezoelectric coefficient detected is d_{33}. This section addresses the problem of the piezoelectric detection if the ferroelectric has an arbitrary orientation.

Given (d^0) the complete set of piezoelectric coefficients for a particular orientation of the coordinates system $S^0 = (x^0, y^0, z^0) = (x^0_i)$ with respect to the principal crystallographic axes, the piezoelectric coefficients along different directions can be calculated using tensor transformations [6,7,182]. For this purpose, a second system of coordinates $S = (x, y, z) = (x_i)$ has to be chosen, in such a way that the directions of interest are along its axes. For example, if only the longitudinal coefficient has to be calculated along a particular direction, then the system *S* is chosen with one of its axis (usually the *z*-axis) to coincide in orientation with the direction of interest. In this case, the *x*- and *y*- axes may have arbitrary orientations, since only the *z*-direction is implied in the measurement (both the electric field and the induced displacement are along *z*). The choice of the system of axes has also to fulfill the condition of being a right-handed orthogonal system. Now the piezoelectric coefficient related to the directions of interest can be computed in the new system of coordinates from the *whole piezoelectric tensor* in the system S^0. For instance, in the aforementioned case, the piezoelectric coefficient d_{33} in the system *S* is the longitudinal piezoelectric coefficient (d_{zz}) along the direction *z* in the system S_0.

The transformation matrix of coordinates from the system S^0 to the system *S* is $A_i^j = a_{ij} = x_i x_j$. The components of the piezoelectric tensor will then transform from the old system to the new one as $d_{ijk} = A_i^m A_j^n A_k^l d_{mnl}^{\upsilon}$. For the compressed (matrix) notation of the coefficients, this transformation become:

$$d = A d^0 N, \qquad \textit{Eq. A 5}$$

where the elements of matrix N are combinations of the elements of the matrix A [7]:

$$N = \begin{bmatrix} a_{11}^2 & a_{12}^2 & a_{13}^2 & a_{12}a_{13} & a_{11}a_{13} & a_{11}a_{12} \\ a_{21}^2 & a_{22}^2 & a_{23}^2 & a_{22}a_{23} & a_{21}a_{23} & a_{21}a_{22} \\ a_{31}^2 & a_{32}^2 & a_{33}^2 & a_{32}a_{33} & a_{31}a_{33} & a_{31}a_{32} \\ 2a_{21}a_{31} & 2a_{22}a_{32} & 2a_{23}a_{33} & a_{22}a_{33}+a_{23}a_{32} & a_{21}a_{33}+a_{23}a_{31} & a_{21}a_{32}+a_{22}a_{31} \\ 2a_{11}a_{31} & 2a_{12}a_{32} & 2a_{13}a_{33} & a_{12}a_{33}+a_{13}a_{32} & a_{11}a_{33}+a_{13}a_{31} & a_{11}a_{32}+a_{12}a_{31} \\ 2a_{11}a_{21} & 2a_{12}a_{22} & 2a_{13}a_{23} & a_{12}a_{23}+a_{13}a_{22} & a_{11}a_{23}+a_{13}a_{21} & a_{11}a_{22}+a_{12}a_{21} \end{bmatrix} \qquad \textit{Eq. A 6}$$

To calculate the longitudinal piezoelectric coefficient along different directions, the new system $S = (x_i) = (x, y, z)$ is rotated in the 3-dimensional space and the d_{zz} coefficient is calculated using Eq. A 5. The system $S^0 = (x^0{}_i) = (x^0, y^0, z^0)$ is chosen with its axes to coincide with the crystallographic ones for which (d^0) is known (for instance [001] is $x^0{}_3$, [100] is $x^0{}_1$, [010] is $x^0{}_2$). A convenient transformation matrix that can be used to rotate the system S in 3-dimensional space with respect to the system S_0 is the following:

$$A = \begin{bmatrix} \sin\varphi & -\cos\varphi & 0 \\ \cos\theta\cos\varphi & \cos\theta\sin\varphi & -\sin\theta \\ \sin\theta\cos\varphi & \sin\theta\sin\varphi & \cos\theta \end{bmatrix}$$

where θ is the angle between the axis z^0 and the axis z, and φ is the angle between the projection of the z-axis on the x^0y^0 plane and the x^0-axis. The transformation matrix A rotates all the three x, y, z-axes but the x-axis is kept in the x^0y^0 plane. The two systems coincide for $\theta = 0°$ and $\varphi = 90°$.

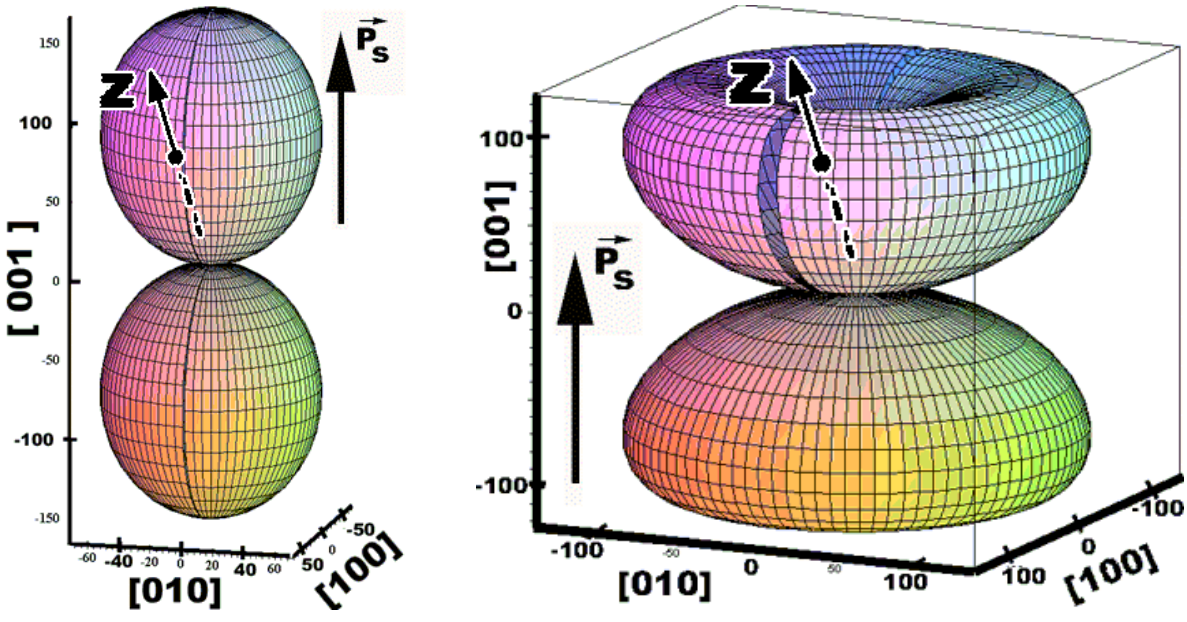

Figure A 4 Longitudinal piezoelectric coefficient d_{zz} (electric field applied along z, displacement measured along z) for the tetragonal symmetry 4mm: **(a)** for PZT(40/60), and **(b)** for $BaTiO_3$. Numerical values used for the calculation are given in Table 2. For the specific meaning of the surface plot see text.

The results of the calculation are shown in Figure A 4 for tetragonal PZT (a) and for tetragonal $BaTiO_3$ (b). In these figures, the distance between one point of the graph and the origin represents the longitudinal piezoelectric coefficient along that direction.

Therefore, if the longitudinal piezoelectric coefficient is not measured along the direction of the spontaneous polarization, the piezoelectric coefficient is not simply proportional to the projection of the polarization on this direction[*]*, but is a complicated function of the other piezoelectric coefficients of the entire piezoelectric tensor.*

By replacing (d^0) in Eq. A 5 with the piezoelectric matrix form of tetragonal single crystals (point group 4mm) the general equation given in Eq. A 7 comes out for the longitudinal piezoelectric coefficient along a direction making the angle θ with the direction of the spontaneous polarization.

$$d_{zz}(\theta) = (d_{31} + d_{15})\sin^2\theta\cos\theta + d_{33}\cos^3\theta \qquad \textit{Eq. A 7}$$

In Eq. A 7 there are two terms that influence d_{zz}. The two materials chosen (Figure A 4) represent the extreme cases for which one of the two terms dominates and determines the shape of the surface: d_{33} in the case of PZT and d_{15} for $BaTiO_3$.

Material (point group)	d_{22}(pm/V)	d_{33}(pm/V)	d_{31}(pm/V)	d_{15}(pm/V)
$BaTiO_3$ (4mm)	-	85	-35	400
PZT (40/60) (4mm)	-	160	-60	170
PZT (60/40) (3m)	75	70	-11	360

Table 2 The piezoelectric coefficients used for the graphic representation (in the standard orientation for each symmetry).

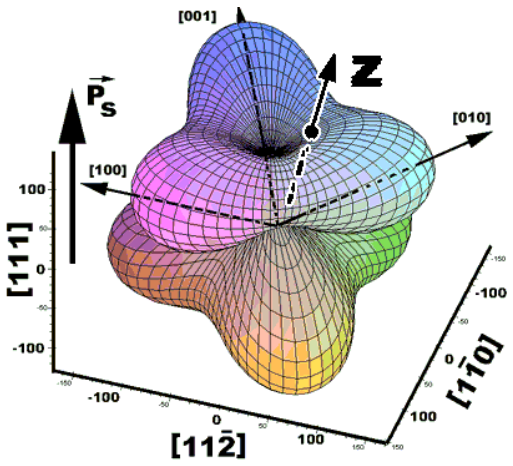

Figure A 5 d_{zz} of rhombohedral PZT. Note that in this case the magnitude of d_{zz} does not reflect anymore the maximum of the *z*-component of the polarization.

[*] for instance, $d_{zz} \neq d_{33}\cos\theta$, where θ is the angle between the directions "*z*" and "*3*".

For lower symmetries, the dependence of the piezoelectric coefficient on the direction is more complex, since there will be more non-zero terms than in Eq. A 7. For example, in Figure A 5 the piezoelectric surface for rhombohedral PZT is given. One can easily notice that the d_{zz} piezoelectric coefficient is not anymore simply related to the component of the spontaneous polarization along the *z*-direction. In such cases, the analysis of the piezoresponse is becoming complex and the images or the local measurements have to be considered with extreme care.

Appendix C: The effective piezoelectric coefficients in thin films – clamping by the substrate

It is well known that piezoelectric measurements of thin films reveal much lower values of the coefficients, compared to the bulk values in standard measurements. This effect has been assigned to the *clamping* of the piezoelectric film by the substrate. The origin of this effect comes from the fact that the longitudinal piezoelectric effect occurs always together with the transversal effect. For the inverse piezoelectric effect, for example, the application of an electric field parallel to $\boldsymbol{P_S}$ does not only cause an extension ($d_{33} > 0$) in the direction parallel to the field, but also a compression perpendicular to the field (d_{31} has almost always a sign opposite to that of d_{33}). If the crystal is not allowed to deform along the transversal directions, then it will deform less along the longitudinal (normal to the film) direction. In the case of thin films on substrates, exactly this is happening, and the direct consequence is that the value of the measured piezoelectric coefficient is much lower than the real one [183].

In the case of the converse piezoelectric effect, the effective piezoelectric coefficient may be easily calculated by using the piezoelectric constitutive equations (Eq. 5a in Sect. 2.2).

In the case of a polycrystalline film poled in the z-direction perpendicular to the film plane, the symmetry class in this case is the same as that for a poled ceramic, i.e. ∞mm . The relevant equations in this case are:

$$D_3 = \varepsilon_{33} E_3 + d_{31}(X_1 + X_2) + d_{33} X_3 \qquad \textit{Eq. A 8}$$

$$\begin{cases} x_1 = s_{11}^E X_1 + s_{12}^E X_2 + s_{13}^E X_3 + d_{31} E_3 \\ x_2 = s_{11}^E X_2 + s_{12}^E X_1 + s_{13}^E X_3 + d_{31} E_3 \\ x_3 = s_{13}^E (X_1 + X_2) + s_{13}^E X_3 + d_{33} E_3 \end{cases} \qquad \textit{Eq. A 9}$$

An ideal clamping in the *x–y* plane (plane of the substrate) implies $x_1 = x_2 = 0$ whereas $x_3 \neq 0$. The symmetry of the film in the plane of the substrate results in $X_1 = X_2$ and because the surface of the film is free, $X_3 = 0$. Eq. A 9 then gives for the effective (measured) converse piezoelectric coefficient in randomly oriented films:

$$d_{33}^{\ clamped} = \frac{x_3}{E_3} = d_{33} - 2d_{31}\frac{s_{13}^E}{s_{11}^E + s_{12}^E} \qquad \textit{Eq. A 10}$$

Since in most materials $d_{31} < 0$ and $s_{13} < 0$, the measured coefficient in films is smaller than in unclamped materials. Therefore, the small values of the piezoelectric coefficients in films relative to the bulk ceramic values can be at least partly explained by the clamping effects of the substrate.

Appendix D: The matrix notation of the electromechanical coefficients

To simplify the notation, the components of the electromechanical tensors (strain, stress, elastic compliance, piezoelectric coefficient, electrostriction, etc) can be written in the matrix (or reduced notation) form, following the Voigt convention given in Table 3. A pair of indices ii = 11, 22, 33, for example, is replaced with the single index m = 1, 2, 3, respectively, and the mixed pairs of indices (which represent shear components of strain and stress tensors) ij = 23 or 32, 13 or 31, 12 or 21 are written as m = 4, 5, 6, respectively.

Tensor notation	Matrix notation
ii = 11, 22, 33	m = 1, 2, 3
ij = 23 or 32, 13 or 31, 12 or 21	m = 4, 5, 6
s_{ijkl}	s_{mn}, both m and n = 1, 2 or 3
2 s_{ijkl}	s_{mn} , m or n = 4, 5, or 6
4 s_{ijkl}	s_{mn} , both m and n = 4, 5, or 6
d_{ijk}	d_{im} , m = 1, 2, 3
d_{ijk}	(½)d_{im} , m = 4, 5, 6
Q_{ijkl}	Q_{ijkl} , m = 1, .., 6, n = 1, 2, 3
2 Q_{ijkl}	Q_{ijkl} , m = 1, .., 6, n = 4, 5, 6

Table 3 Conventions for the matrix notation